

Article

Spatial Distribution and Structural Characteristics for *Haloxylon ammodendron* Plantation on the Southwestern Edge of the Gurbantünggüt Desert

Chunwu Song^{1,2,3}, Congjuan Li^{2,3,*}, Ümüt Halik^{1,4,*} , Xinwen Xu², Jiaqiang Lei², Zhibin Zhou² and Jinglong Fan²

¹ College of Resource & Environment Sciences, Xinjiang University, Shengli Road 666, Urumqi 830046, China; songcw@ms.xjb.ac.cn

² National Engineering Technology Research Center for Desert-Oasis Ecological Construction, Xinjiang Institute of Ecology and Geography, Chinese Academy of Sciences, Urumqi 830011, China; sms@ms.xjb.ac.cn (X.X.); desert@ms.xjb.ac.cn (J.L.); zhouzb@ms.xjb.ac.cn (Z.Z.); fanjl@ms.xjb.ac.cn (J.F.)

³ Mosuowan Desert Research Station, Xinjiang Institute of Ecology and Geography, Chinese Academy of Sciences, Mosuwan 832056, China

⁴ Ministry of Education Key Laboratory of Oasis Ecology, Xinjiang University, Shengli Road 666, Urumqi 830046, China

* Correspondence: licj@ms.xjb.ac.cn (C.L.); halik@xju.edu.cn (Ü.H.)

Abstract: *Haloxylon ammodendron* (C.A.Mey.) Bge. is crucially important for stabilizing sand dunes in the desert area of the Junggar Basin and has thus been widely planted in the oasis–desert ecotone for windbreak and sand fixation purposes since the 1980s. The spatial distribution and structural characteristics of *Haloxylon ammodendron* plantations of three different ages—planted in 1983 (36a), 1997 (22a), and 2004 (15a)—on the southwestern edge of the Gurbantünggüt Desert were studied. The results showed that the spatial distribution patterns for the different stages of growth showed a trend of cluster that was random during the transformation from seedlings to juvenile and mature trees. Forest density for the 15a, 22a, and 36a plantations was, respectively, 1110, 1189, and 1933 plants ha⁻¹; the base stem diameter for the main forest layer was 5.85, 8.77, and 6.17 cm, respectively, and the tree height was concentrated in the range of 1.5–3.0 m, 2.0–3.5 m, and 1.5–2.5 m. In the regeneration layers, the proportion of seedlings was the largest in all three stand ages, followed by juvenile trees, and mature trees only appeared in the 22a plantation. The proportion of deadwood in the 36a forest was the highest, and there were no mature trees in the regeneration layer. These results indicate that the three *Haloxylon ammodendron* plantation stages were in the period of rising at 15a, stable and degenerate with increasing age at 22a, and at 36a the regeneration ability was very weak and presented degradation due to species competition for soil moisture, because of too many seedlings and mature plants. In this case, measures such as thinning could be taken to prevent rapid degradation and to accelerate regeneration when the stand age exceeds 20 years. Considering the sand fixation effect, the pressure of competition for water resources, and forest capacity for renewal and sustainability, the most suitable forest density in the *Haloxylon ammodendron* plantation would be 8.5–9 m² per plant.

Keywords: spatial patterns; population dynamics; planting density; *Haloxylon ammodendron* plantation



Citation: Song, C.; Li, C.; Halik, Ü.; Xu, X.; Lei, J.; Zhou, Z.; Fan, J. Spatial Distribution and Structural Characteristics for *Haloxylon ammodendron* Plantation on the Southwestern Edge of the Gurbantünggüt Desert. *Forests* **2021**, *12*, 633. <https://doi.org/10.3390/f12050633>

Academic Editor: Timothy A. Martin

Received: 19 April 2021

Accepted: 12 May 2021

Published: 17 May 2021

Publisher's Note: MDPI stays neutral with regard to jurisdictional claims in published maps and institutional affiliations.



Copyright: © 2021 by the authors. Licensee MDPI, Basel, Switzerland. This article is an open access article distributed under the terms and conditions of the Creative Commons Attribution (CC BY) license (<https://creativecommons.org/licenses/by/4.0/>).

1. Introduction

Arid areas make up about 30% of China's total territory and are expanding every year [1]. The oasis-desert ecotone plays an important ecological role in the arid region and is characterized by sparse vegetation, shortage of water resources, and fragile environment [2]. Ecological protective projects have been effectively established in China to protect the oasis-desert ecotone, which is itself essential for protecting the ecological environment and maintaining the stability of the oasis [3].

As the largest and most concentrated species in the Gurbantünggüt Desert, *Haloxylon ammodendron* forest acts as a natural barrier protecting the edge of the oasis from sandstorms [4]. However, excessive logging, grazing, and unreasonable reclamation during the 1970s and 1980s caused serious damage to the natural *Haloxylon ammodendron* forest within 20–50 km of the Junggar Basin. In the 1980s, the area of *Haloxylon ammodendron* forest was only 68.4% of that occupied in 1958 [5].

Haloxylon ammodendron is a dominant xerophyte species of large ecological importance in stabilizing sand dunes [6]. As an excellent biological sand fixation species, *Haloxylon ammodendron* has strong adaptability and tolerance to high temperature, drought, and salinity in desert ecosystems [7,8], and it has been the preferred tree species for artificial afforestation around the Junggar Basin since the 1980s [9]. The sand-fixing system established in the Mosuowan reclamation area and the Manas River Basin has been viewed as a successful model of artificial ecological engineering in desert regions [10,11]. However, artificial vegetation in the Mosuowan region is characterized by single-species plantations of high density and is experiencing varying degrees of decline after nearly 40 years [12]. Hence, it is necessary to clarify the spatial patterns of plant populations and the reasons for the decline of plantations.

Spatial patterns of plant populations are closely related to ecological processes [13–15]. Spatial distribution patterns and interactions play a major role in explaining the coexistence of species, the relationship between species and habitat, and the ecological processes of populations [16,17]. For example, clustered spatial distribution patterns of vegetation may result from heterogeneous microhabitats, facilitative interactions, or local seed dispersal, while uniform spatial patterns may indicate homogeneous habitat conditions [18–21]. Spatial interactions help to reveal the complex balance between competition and facilitation, and demonstrate how competition and facilitation exist simultaneously—for example, under favorable environmental conditions, competition predominates, while under stressful conditions, facilitation prevails—and different spatial interactions may result in specific spatial patterns [22,23]. Increased understanding of spatial distribution patterns and interactions may provide insights into forest succession as well as give early warning signs of vegetation degradation [24–27].

The transitional regions between oases and deserts with fragile ecosystems are related to the ecological security of the oasis [28–30]. Investigating the characteristics and spatial patterns of artificial sand-fixing plants contributes to exploring the main causes of vegetation degeneration, and the evolutionary processes and driving mechanisms of artificial sand-fixation plants, and would provide reference for plantation construction and management in other oasis-desert ecotones [31].

The Junggar Basin, located in Northern Xinjiang, is recognized as one of the world's most sensitive regions to global change [32]. The Mosuowan reclamation area is located in the southwestern margin of the Junggar Basin. There is stable snow cover in this area in winter, with a maximum snow thickness of more than 20 cm. Melting snow in early spring provides favorable conditions for the growth and development of desert plants [33,34]. *Haloxylon ammodendron* is one of the most important and commonly used sand-fixing species in the Junggar Basin [35], the distribution area of which in Xinjiang is account for 68.1% of the total area of China [36]. While investigating the characteristics and spatial patterns of artificial sand-fixing plants contributes to exploring the main causes of vegetation degeneration, this case would also be beneficial for further study of the evolutionary processes and driving mechanisms of artificial sand fixation plants, and would provide some reference for plantation construction and management in other oasis-desert ecotones.

The specific objectives of this study were to: (1) determine whether the artificial *Haloxylon ammodendron* forest experience a recession with the increasing of stand age? (2) explore the main reasons for the recession and to provide theoretical basis for the renewal and sustainable development of artificial shelterbelt in this area.

2. Materials and Methods

2.1. Study Area

This study is centered on the intersection of oasis-desert on the southwestern edge of the Gurbantünggüt Desert, near the Mosuowan Desert Research Station (86°1' E, 45°7' N) of the Xinjiang Institute of Ecology and Geography, Chinese Academy of Sciences (Figure 1). This area is a typical temperate arid desert. The annual average precipitation is less than 120 mm, as shown by the 1980–2007 precipitation presented in Figure 2, and the annual evaporation is about 2000 mm; precipitation is mostly concentrated in winter and spring [37,38]. The average annual temperature is 6.6 °C, with a mean maximum above 40 °C in July and a minimum of less than −40 °C in January. The groundwater depth decreased from 8 m in 1998 to 12 m in 2007, and it is still declining at a rate of 0.35 m per year [39,40].

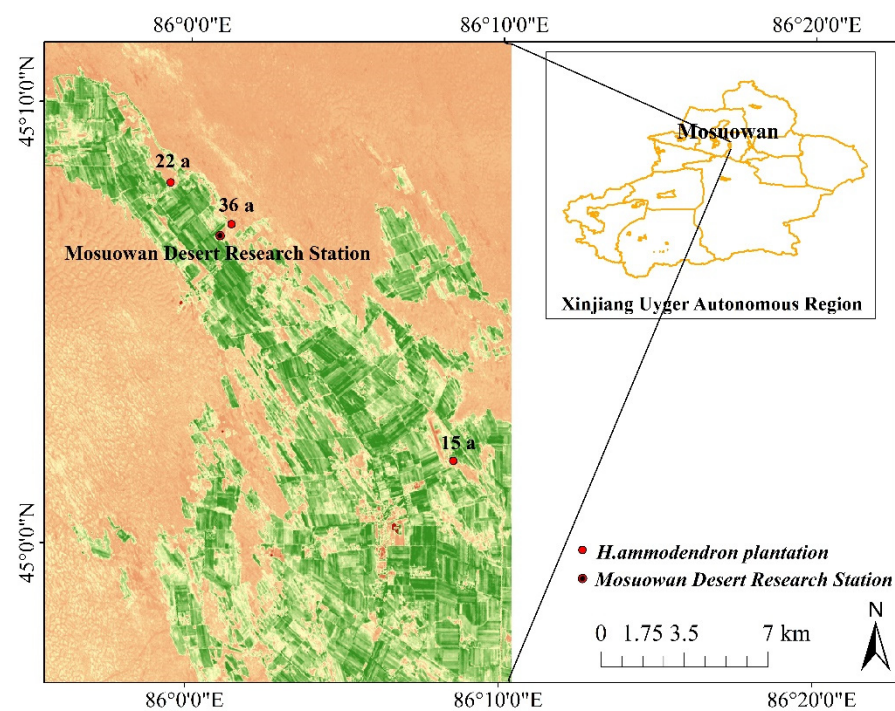


Figure 1. Location of the study sites in the Mosuowan reclamation area.

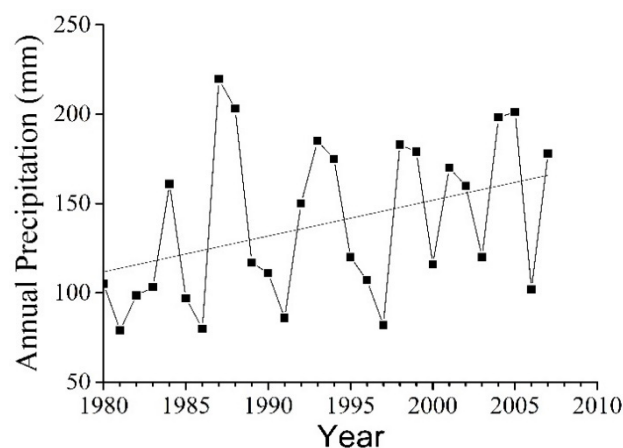


Figure 2. Annual precipitation at the study sites in the Mosuowan reclamation area.

The study area is located in the fine soil plain of the oasis-desert ecotone. The soil is sandy loam. The 0–100 cm vertical direction layers of the soil have average percentage

contents of clay (<0.002 mm), powder (0.002–0.05 mm), and sand (0.05–2 mm) of 3.12%, 32.63%, 64.25% respectively. The vegetation cover of the study area is ~20–30%, and the dominant species is *Haloxylon ammodendron* accompanied by a few other species such as *Tamarix chinensis*, *Calligonum leucocladum*, and *Nitraria sibirica* [41,42]. Single *Haloxylon ammodendron* species were planted at different stages, spaced 3 m in rows and 1 m in columns, to prevent the desert spreading to the oasis.

2.2. Field Investigation

In 2019, three plots of different planting stages, from 1983 (36a), 1997 (22a), and 2004 (15a), were selected for investigation in the study area. These were chosen with consideration of the appropriate scale for structure-related and spatial-pattern study [43] and of the consistency of the plot sizes at different stages, based on the study of spatial scale of shrubs by Zuo and Zheng [21,44], a 50 m × 60 m survey plot was selected for each site. The selected plots are uniform in topography and are not disturbed by grazing and logging. No other artificial tending measures such as fertilization, irrigation, or pruning were adopted after the afforestation project had been completed for all plots. The DGPS global positioning system (iHand A10, DGPS) was used to determine the coordinate information (x, y coordinates) of all living trees in each plot. The investigation parameters included plant height, crown width, base stem diameter, and relative proportions of dead branches.

The vertical structure of the *Haloxylon ammodendron* plantations can be divided into two layers: main forest layer and regeneration layer. The main forest layer is the *Haloxylon ammodendron* plantation, and the regenerated layer includes all naturally regenerated seedlings and saplings in the stand [12]. Additionally, the individual plants in the regeneration layer are divided, according to their ground stem, into seedlings (<1.2 cm), saplings (>1.2 cm and <6.5 cm), and mature trees (>6.5 cm) [45,46].

2.3. Data Analysis

R software was used to analyze the spatial distribution patterns of *Haloxylon ammodendron* in each plot. Plants are represented as points and are mapped individually with Cartesian coordinates within a plot [47–49]. The L-function of univariate spatial analysis was chosen to describe the spatial patterns of all trees in the three developmental stages. The L-function [50] is derived from the Ripley's K-function [51]. An approximate variance-stabilizing transformation for the K-function is the square root. The L-function stabilizes and linearizes the variance of the K-function, which simplifies the interpretation of results. The edge-effect correction method can be applied for rectangular study areas extended by Goreaud and Pelissier based on Ripley's local weighting factor [52]. So, spatial patterns can be described as random, regular, or aggregated, respectively, when the values of $L(r)$ fall within, below, or above the confidence envelope [53]. The univariate estimators of the K- and L-functions are calculated as:

$$K(r) = \frac{A}{n^2} \sum_{i=1}^n \sum_{j=1}^n w_{ij}^{-1} I_r u_{ij} \quad (1)$$

$$L(r) = \sqrt{\frac{K_r}{\Pi}} - r \quad (2)$$

where A is the area of the plot; n is the number of trees; u_{ij} is the distance between two points i and j ; $I_r u_{ij}$ is the indicator function, $I_r u_{ij} = 1$ if $u_{ij} \leq r$, when $u_{ij} > r$, $I_r u_{ij} = 0$; and w_{ij} is the weight value for edge correction [54].

SPSS (version 20.0, IBM, New York, NY, USA.) software were used for statistical analysis. The base diameter and height of the main forest layer were completed using Origin (version 9.1, OriginLab, Northampton, MA, USA). The spatial analysis L-function was completed using the "spatstat" package of the statistical software package R [55]. The spatial distribution map of basal stem diameter was completed by the "ggplot2" package of the statistical software package R [21]. Semivariance analysis was used to further describe

the spatial dependence of plant populations, and the geostatistical analysis was completed with the software package GS + version 7 (Mail Gamma Design Software, LLC, Plainwell, MI, USA).

3. Results

3.1. Basic Characteristics of *Haloxylon ammodendron* Plantations

There were significant differences in the basic characteristics of plantations between different developmental stages (Table 1). The survival rate of the main forest layer was 30.4%, 17.7%, and 55.9%, respectively, for the 15a, 22a, and 36a plots. The deadwood proportion presented a trend similar to the survival rate with increasing forest age, reaching 41.15% at the 36 years stage. The height, crown width, and basal stem diameter all present trends that increase then decrease with increasing forest age. The average basal stem diameter and height at 36a were 6.17 cm and 2.59 m, which were smaller than 8.77 cm and 4.51 m at 22a.

Table 1. Basic characteristics of the main forest layer at different stand ages.

Traits	15a Initial Column and Row Spacing (m): 1 × 3	22a Initial Column and Row Spacing (m): 1 × 3	36a Initial Column and Row Spacing (m): 1 × 3
Number of current individuals	304	177	559
Density/individual (m ²)	0.104	0.059	0.186
Survival rate (%)	30.4	17.7	55.9
Height (cm)	235.49 ± 78.91	289.44 ± 91.79	200.66 ± 52.32
Crown width (m ²)	3.41 ± 0.61	4.51 ± 0.69	2.59 ± 0.39
Base stem diameter (cm)	5.85 ± 2.61	8.77 ± 3.42	6.17 ± 2.46
Deadwood proportion (%)	29.70 ± 25.65	15.65 ± 15.76	41.15 ± 23.79

The semi-variance analyses of height, crown width, diameter of base stem, and the deadwood proportion in *Haloxylon ammodendron* in the three stages are shown in Figure 3. The semi-variance function can be simulated by exponential and spherical models respectively. The semi-variance function values of each of the indicators in 15a increased rapidly with the increase of distance in the range of 0–5 m, then became stable in the 5–30 m range, and decreased with the increase of distance in the 30–40 m range. For the 22a plot, the indicators increased rapidly with the increase of distance in the range of 0–40 m. In the 36a plot, all values increased rapidly in the range of 0–5 m and reached a relatively stable situation after 5 m. Additionally, the 22a plot showed high variation in tree height, crown width, diameter at the base stem, and deadwood proportion, indicating strong patch patterns. The results show that the degree of spatial heterogeneity in the three stand stages is 15a < 22a < 36a.

3.2. Structural Characteristics of the Main Forest Layer

The diameter class distribution of *Haloxylon ammodendron* in the main forest layer showed the trend of concentration–dispersion–concentration with the increase of stand age. The basal stem diameter of 15a stands ranged mostly from ~2–4 cm, 4–6 cm, to ~6–8 cm, with the majority of individuals measuring ~2–8 cm, accounting for 74.67% of the total. The basal stem diameter class width of 22a was divided into seven, with the stem diameter distribution becoming obviously loose; however, the proportion of individuals with a diameter of ~6–12 cm was the largest (58.76%). The basal stem diameter class width of 36a was also divided into seven, although the center of diameter distribution moved down to ~4–10 cm (76.03%). The results showed that the main forest layer appeared to differentiate after ten years of growth. The growth of the base diameter of the main forest layer of *Haloxylon ammodendron* can therefore be divided into three periods: growth rising stage (15a), growth stabilization stage (22a), and growth decline period (36a).

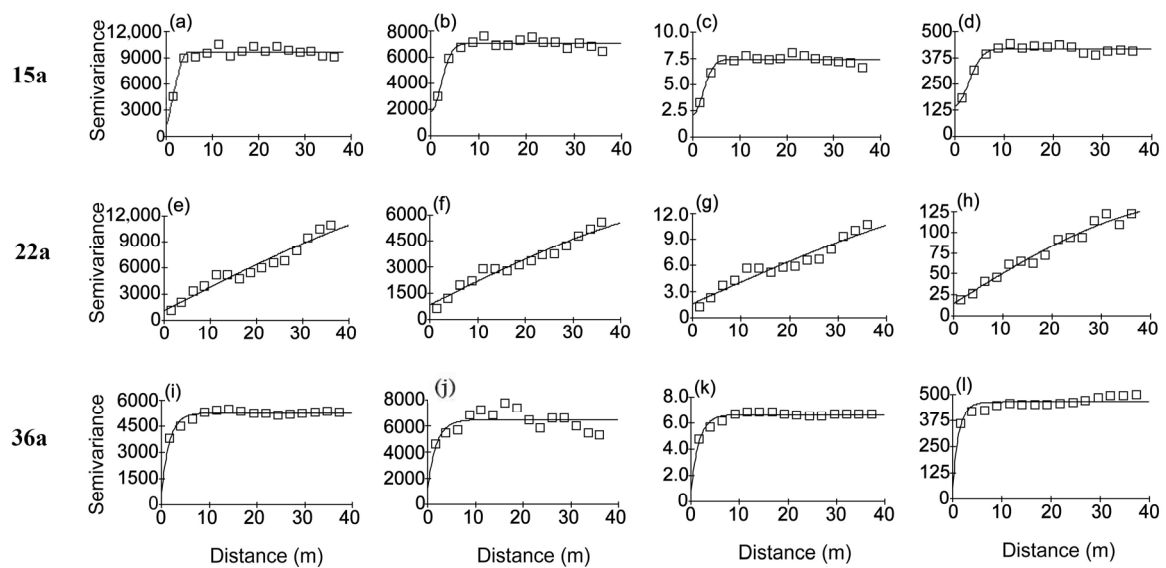


Figure 3. Semi-variograms for height (a,e,i), crown width (b,f,j), diameter of base stem (c,g,k), and deadwood proportion (d,h,l) of *Haloxylon ammodendron* plantations of different stand stages at 15a, 22a, and 36a, respectively.

The height of the main forest layer in *Haloxylon ammodendron* plantations shows a similar trend to the base diameter (Table 1; Figure 4). The tree height class of 15a is relatively concentrated. Although it includes 11 tree height classes, most individuals are concentrated in the ~1.5–3.0 m segments, which account for up to 66.45%. For the 22a plot, ten height classes were presented with relatively scattered distribution, although mainly concentrated in the range of ~2.0–3.5 m, which accounts for up to 61.02%. In the 36a plot, the tree height center has moved down to the ~1.5–2.5 m segments, which account for up to 79.57%, and indicate that the center of height was declining. The growth trend of height in the main forest layer therefore also showed a trend of growth, stability, and decline.

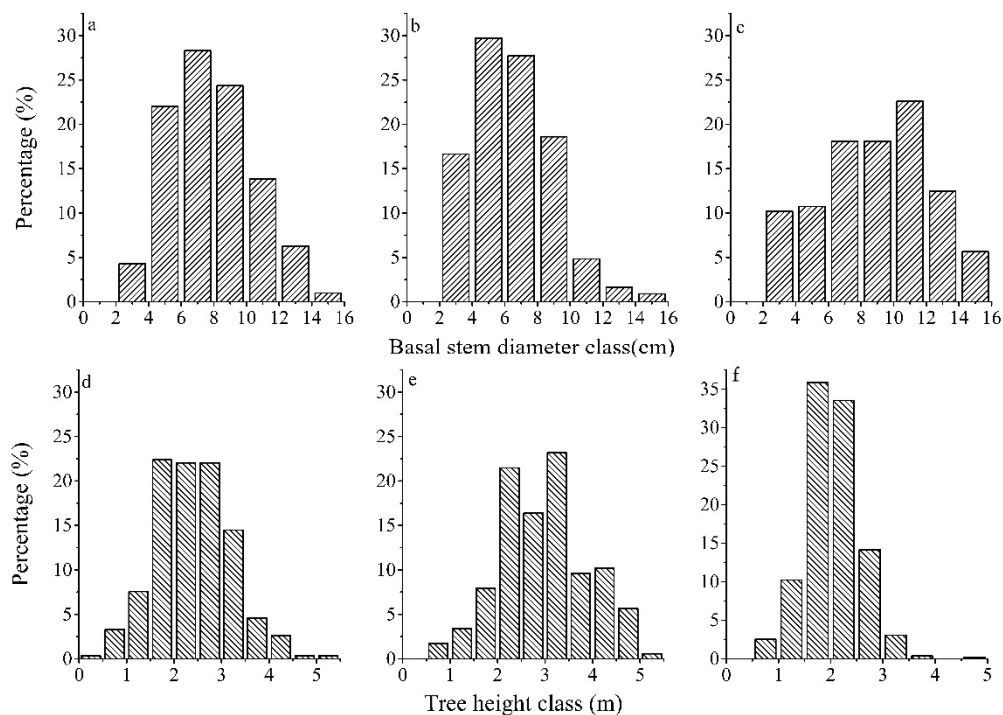


Figure 4. Basal stem diameter and tree height characteristics of the main stand layer of *Haloxylon ammodendron* plantations of different stand ages: Basal stem diameter class (a, 15a; b, 22a; and c, 36a), tree height class (d, 15a; e, 22a; and f, 36a).

The density distribution contour map of the deadwood proportion was drawn using the Kriging interpolation algorithm (Figure 5). It can be seen from the figure that in the 15a plot, 0–40% of deadwood proportion accounts for more than 85% of the total; in the 22a plot, 0–20% of deadwood proportion accounts for more than 91%; and in the 36a plot, 20–60% accounts for more than 93%. According to the average proportion of dead branches, in the 15a plot the deadwood proportion reached 29.7%, the 22a plot was 15.65%, and 36a was 41.15% (Table 1). The deadwood proportion shows a trend of first decreasing, and then increasing with the increase of forest age.

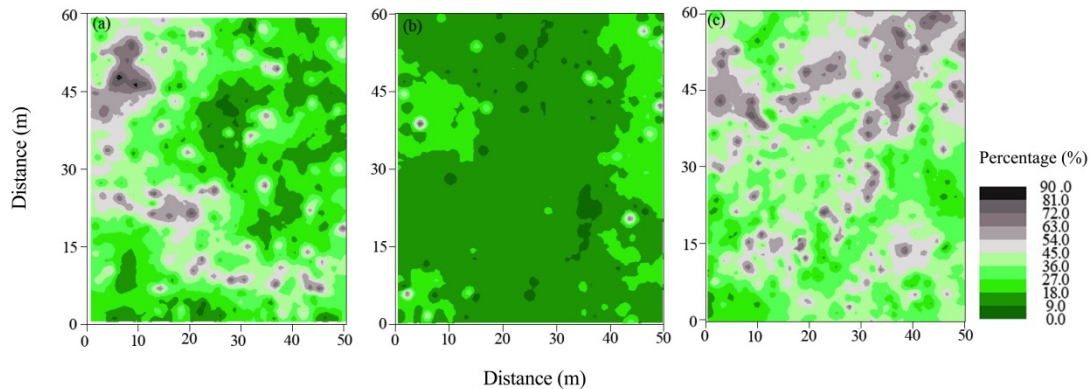


Figure 5. The deadwood proportion of the main forest layer in *Haloxylon ammodendron* plantations of different stand ages: (a), 15a; (b), 22a; and (c), 36a. Different colors represent the deadwood proportion of individual trees.

3.3. Structural Characteristics of the Regeneration Layer

The tree density of the regeneration layer in the 15a stage plot was 3226 plant ha⁻¹, with seedlings, juvenile trees, and mature trees accounting for 97.73%, 2.27%, and 0%, respectively (Table 2; Figure 6). The stage has a stable seedling regeneration ability, while the regeneration ability of juvenile trees is rather weak, resulting in no mature individuals. For the 22a stage, the individuals increased to 7120 plant ha⁻¹, with seedlings, juvenile trees, and mature trees accounting for 91.39%, 7.96%, and 0.65%, respectively. At the 36a stage, the plant individuals had increased to 7423 plant ha⁻¹, with seedlings, juvenile trees, and mature trees accounting for 99.07%, 0.93%, and 0%, respectively. While there is obvious seedling regeneration, the number of juvenile trees is very small, and these did not grow into mature trees. All three stand ages showed good seedling renewal status. In the 22a stage plot, juvenile trees and mature trees were present in the regeneration layer.

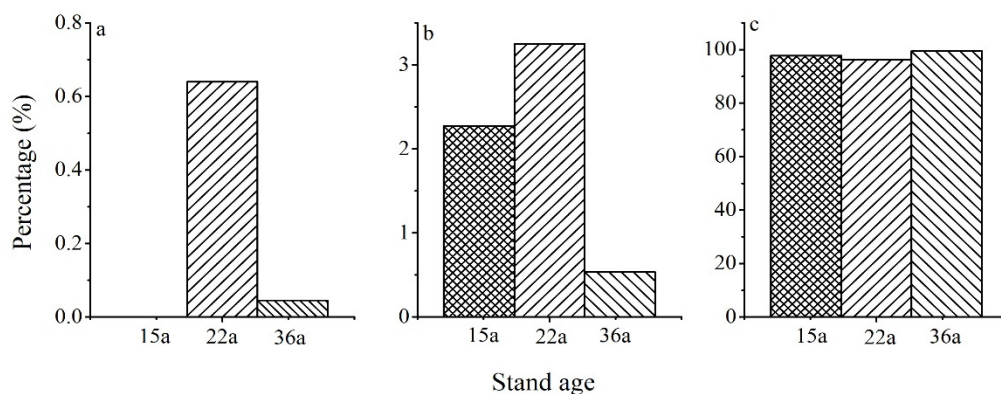


Figure 6. Basal stem diameter structure of the regeneration layer in *Haloxylon ammodendron* plantations at different stand ages. Stand age: (a) for mature >6.5 cm; (b) for juvenile >1.2 cm and <6.5 cm; (c) for seedling <1.2 cm.

Table 2. Basic characteristics of the regeneration layer at different stand ages.

Traits	15a			22a			36a		
	Seedling	Juvenile	Mature	Seedling	Juvenile	Mature	Seedling	Juvenile	Mature
Survival	946	22	/	1952	170	14	2227	21	/
Frequency (%)	97.73	2.27	0	91.39	7.96	0.65	99.07	0.93	0
Density (m ²)	0.315	0.007	/	0.651	0.057	0.005	0.742	0.007	/
Height (cm)	20.79 ± 12.11	91.36 ± 27.18	/	21.29 ± 15.86	142.79 ± 50.11	211.07 ± 36.38	32.14 ± 13.56	73.52 ± 30.36	/
Crown width (m ²)	0.015 ± 0.015	0.47 ± 0.06	/	0.013 ± 0.014	0.64 ± 0.13	0.94 ± 0.16	0.039 ± 0.014	0.19 ± 0.049	/
Base diameter (cm)	0.28 ± 0.21	1.42 ± 0.34	/	0.27 ± 0.19	2.58 ± 1.42	10.04 ± 3.74	0.39 ± 0.18	1.67 ± 0.52	/

3.4. Spatial Patterns of *Haloxylon ammodendron* Individuals at Different Forest Ages

The spatial patterns of *Haloxylon ammodendron* at three stages of development are shown in Figure 7. The left-hand column presents maps showing the locations of individual trees. The size of the trees is indicated by symbols sized in proportion to the diameter of the base stem. The right-hand column shows univariate results from the L-function—plots of L-functions against distance that are below the lower confidence interval indicate discrete spatial patterns, while those that are above the upper interval indicate clustered patterns, and those within the confidence intervals indicate random spatial patterns. The results indicate that trees in the 15a stage showed clustered patterns when the distance was >2 m. Trees in the 22a stage were randomly distributed at distances of 1–12 m, and aggregated when the distance was <1 m. Additionally, in this stage the forest gap appeared due to enhanced self-thinning and alien-thinning of the *Haloxylon ammodendron* plantation, which creates the conditions for seedlings to grow into juvenile and then mature trees. Trees in the 36a stage were randomly distributed when the distance was >2 m and also aggregated when the distance was <2 m. The self-thinning effect of the *Haloxylon ammodendron* population did not increase significantly. The *Haloxylon ammodendron* plantation at this stage is in obvious decline; there is no evident forest gap, so the individual competition of the large basal stem diameter of the main forest layer is still strong.

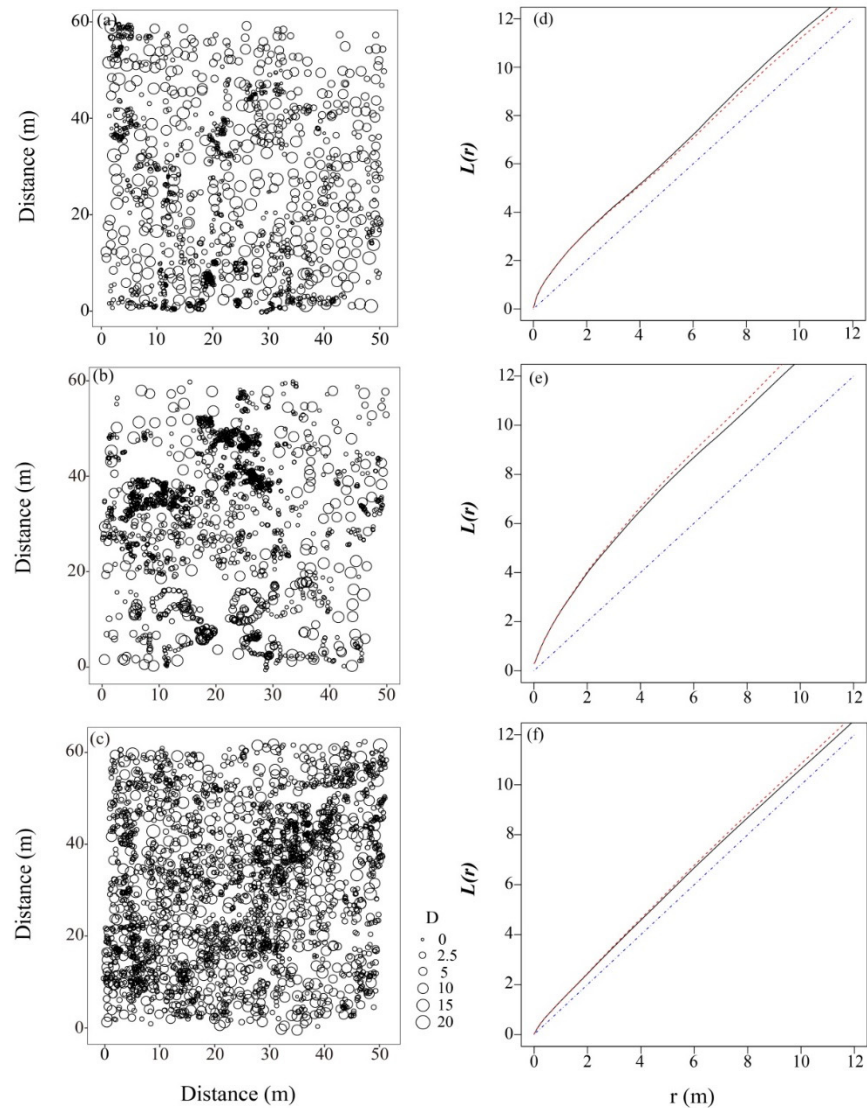


Figure 7. Stem maps (a, 15a; b, 22a; and c, 36a) and spatial patterns (d, 15a; e, 22a; f, 36a) of *Haloxylon ammodendron* at three stages of development.

4. Discussion

4.1. Growth Dynamics of the *Haloxylon ammodendron* Plantations

The survival rate of the main forest layer at different forest ages is significantly different. The 36a survival rate is the highest, at up to 55.9%, and the 22a survival rate is the lowest, results which are inseparable from local precipitation and soil water content factors [34]. Heat surplus and water deficiency are one of the important natural characteristics in arid areas, the water balance of soil is the main factor restricting the growth and renewal of desert vegetation [9]. Snow water supply in early spring is the main environmental factor affecting the survival of seedlings of *Haloxylon ammodendron* [56]. Therefore, the precipitation at the planting year is one of the main factors affecting the final survival rate of *Haloxylon ammodendron* plantation.

With the increase of the age of *Haloxylon ammodendron* plantation, the competition within the main forest layer is increasing, and the emergence of regeneration layer seedlings make the population structure more complex [12]. The height and diameter class structure of 22a was more differentiation than 35a, and the population structure was more single and the deadwood proportion in 35a plot is the highest. The population structure is characterized by rapid change in the early stage, stable in the middle stage and decline in the later stage. Li obtained the same conclusion about growth trend by used different stem-level structure to represent the stand age of *Haloxylon ammodendron* plantation [57]. Therefore, this included that the *Haloxylon ammodendron* can be divided into three periods of growth rising stage (15a), growth stabilization stage (22a) and growth decline period (36a), respectively.

The tree height and the basal stem diameter structure of the main forest layer showed obvious differentiation in the 22a plot, with the results showing that, after the competition and self-thinning stage, some dominant individuals entered the stage of rapid growth, while others with weak competitiveness were in the stage of slow growth. The tree height and base diameter mostly concentrated at ~3–3.5 m and ~8–10 cm, respectively, which reflected that there are more individuals in the upper canopy of the main forest layer, and most of the individuals can grow to the forest canopy layer. In the 36a plot, tree height and base stem diameter obviously stagnated or even returned to a smaller value than the 22a stage (Figures 3 and 4). This phenomenon may be principally due to rodent damage, since our investigation found that the young branches of whole trees had been bitten off by rats. Additionally, the survival rate both in the main forest layer and the regeneration layer of the 36a plot were both higher than in the 22a plot, which inevitably increased interspecies competition and restricted the growth of individual plants [58,59].

In the regeneration layer, the density of seedlings was greatest in the 36a plot, while the transformation of seedlings to juvenile trees was quite low, with no mature trees appearing. This characteristic reflects the obvious decline of reproductive growth of the *Haloxylon ammodendron* 36a plantation, while the preservation rate and canopy density of the stand remain high, providing a great obstacle for the seedlings to grow into juvenile or mature trees. In the 22a plot, seedling density in the regeneration layer was slightly lower, but the ratio of seedling growth to juvenile trees and mature trees was the highest, mainly because significant forest gaps were presented (Figure 5). In the process of stand succession, some individuals of *Haloxylon ammodendron* died due to the change of local precipitation or microenvironment, or interspecies competition resulting in forest gaps, which provided favorable conditions for the regeneration-layer seedlings to grow into mature trees [60].

Plant regeneration is the process from seed generation, diffusion, germination, and seedling formation to juvenile tree construction, and seedlings are a potential regeneration pool for population succession [61]. In this study, the proportion of seedlings in the regeneration layer were the greatest in all three stand ages, and these sufficient seedling pools can provide a strong guarantee for the regeneration and succession of the population [21]. However, natural regeneration is not simple replacement, and the continued existence of a large seedling bank cannot guarantee good regeneration [12]. Sufficient juvenile or mature trees are the key to ensure the natural regeneration and sustainable development

of the *Haloxylon ammodendron* plantations. This study shows that the growth of larger individuals (juvenile and mature trees) in the regeneration layer was good in the 22a stand, which indicated that the *Haloxylon ammodendron* plantation had the potential for continuous regeneration and succession under this environment. However, limitation factors such as drought and water shortage may always restrict the emergence, settlement, and growth of regeneration individuals [21]. So, artificial management intervention would be beneficial for the sustainable regeneration of stands.

4.2. Spatial Patterns of the *Haloxylon ammodendron* Plantations at Different Stand Ages

The univariate spatial analyses clearly revealed the different spatial patterns of *Haloxylon ammodendron* plantations at the different stand ages. At large scales (>2 m), cluster patterns were present in the 15a stage, and random distributions occurred in the 22a and 36a stages. At small scales (<1–2 m), random patterns were present in the 15a stage, and cluster distributions occurred in the 22a and 36a stages. These results were consistent with the former study by Stoll and Bergius [20], which found that the spatial distribution of conspecifics under tree-size asymmetrical competition can shift from initially clustered, via random, to regular, as a result of density-dependent mortality. At the same time, these results were different from the former study which documented that spatial patterns of *Haloxylon ammodendron* plantations in Minqin of 30–40 years and >40 years were in the clustered mode [21]; this can be interpreted as the obvious self-thinning and decline of the Minqin *Haloxylon ammodendron* plantation over 30 years. While the main forest layer of the 36a plot of *Haloxylon ammodendron* plantation in Mosuowan did not show obvious self-thinning, and the survival rate was high, it can be seen from the distribution map of the deadwood proportion that this is highest in the 36a stage, indicating that the high survival rate is not conducive to plant succession and renewal.

L(r)-function showed that the distribution of the *Haloxylon ammodendron* plantations presented a clustered—random trend during the transformation from seedlings and juvenile trees to mature trees. This was similar to the findings of a former study in the Gurbantünggüt Desert [4,29]. The 22a stage exhibited high variation in all four variables, while the changes in 36a were the most gentle, followed by 15a. Additionally, the variation of 22a was significantly higher than that of the other two stand ages, at two to three times the others, which showed that the spatial heterogeneity was highest in the 22a plot.

4.3. Main Factors Affecting the Spatial Patterns

Spatial patterns of plant populations are the result of the combined effects of localized dispersal, abiotic stresses, biotic interactions, and disturbance [62]. In this study, the main factors affecting the spatial patterns were the interactions between conspecifics and abiotic heterogeneity. While water shortage is one of the important natural features in arid desert areas, the water balance of the soil is the main factor for restricting the growth and regeneration of desert vegetation [9]. So, the soil moisture is the main environmental factor affecting the survival of seedlings in *Haloxylon ammodendron* plantations [63].

Soil water balance is thus the main factor restricting the growth and regeneration of desert vegetation [64]. Although *Haloxylon ammodendron* is much more tolerant to water shortage than other plants, soil moisture is still the main environmental factor for the survival of its seedlings and the sustainable development of plantations [65]. The water use strategies of different ages of *Haloxylon ammodendron* are different [34]. Seedlings mainly use surface water and 150 cm surface soil water, while trees of ten or more years mainly use 150–200 cm soil water and groundwater, and those of 20–30 years mainly use groundwater [66]. So, no competition for surface water will ensure a large number of seedlings in the plantation, while young trees and mature trees will compete with the main forest layer for water [67]. However, the seedlings that are most sensitive to environmental changes are strongly screened by water-dominated environmental factors and often die before growing to the juvenile or mature stage [42]. Therefore, in the desert area around Junggar Basin, measures such as thinning would prevent the rapid decline of *Haloxylon*

ammodendron plantations and accelerate regeneration. From Table 3, the initial planting density in this area can be considered to be no more than 3333 plants ha⁻¹ (row spacing of 3 m × 1 m), which is more than the number given in a former study of 1666 plants ha⁻¹ [11].

Table 3. Survival characteristics of *Haloxylon ammodendron* plantations at different stand ages.

Number of Individual Trees	15a	22a	36a
Main forest layer	304	177	559
Regeneration layer (Juvenile)	22	170	21
Regeneration layer (Mature)	0	14	0
Total in plot	326	354	580
Initial plant density (plant ha ⁻¹)	3333	3333	3333
Preservation Density (plant ha ⁻¹)	1086	1180	1933

5. Conclusions

In the past few decades, *Haloxylon ammodendron* plantations of different forest ages have undergone different processes of succession. They were initially planted uniformly, but declined to different degrees and resulted in non-uniform spatial patterns, which resemble as the natural vegetation, with the representative self-organized characteristics of patchy distribution. The characteristics of the main stand layer and the regeneration layer may provide direct and comprehensive knowledge for the healthy development of a sand-fixing plantation. Promoting natural regeneration can greatly reduce the cost of regeneration. When the age of the plantation is more than 20 years, or where no juvenile or mature trees have appeared in the forest, pruning measures can be taken to control stand canopy density and promote the regeneration of seedlings to form a more stable structure in ecological function. When the age is more than 30 years, intercropping measures can be taken to alleviate degeneration and promote the renewal of juvenile and mature trees to complete the gradual replacement of the old ones. Ultimately, the preferable initial planting density of the *Haloxylon ammodendron* plantations (3333 plants ha⁻¹) is basically reasonable in the Mosuowan reclamation area. Additionally, the expected effects optimum pruning and intercropping measures in the later stage will prolong the ecological service period of the *Haloxylon ammodendron* plantations in the oasis-desert ecotone.

Author Contributions: X.X., Z.Z., J.L. and C.S. conceived the ideas and designed this study; C.S., C.L. and J.F. interpreted the data of spatial distribution and structure characteristics and analysis; C.S. wrote the manuscript; C.L. and Ü.H. reviewed the manuscript. All authors have read and agreed to the published version of the manuscript.

Funding: This research was supported by the National Natural Science Foundation of China (31971731, 41771121), the Xinjiang National Key Research and Development Program (2019B00005), the K.C. Wong Education Foundation, and the Youth Innovation Promotion Association of the Chinese Academy of Sciences (2017476).

Acknowledgments: We thank Guangming Chu, Bowen Zheng for providing us the data monitoring and Baijun Shang for revising some of the figures.

Conflicts of Interest: The authors declare that they have no known competing financial interests or personal relationships that could have appeared to influence the work reported in this paper.

References

1. Adeel, Z. Findings of the global desertification assessment by the Millennium Ecosystem Assessment—A perspective for better managing scientific knowledge. In *The Future of Drylands*; Lee, C., Schaaf, T., Eds.; Springer: Dordrecht, The Netherlands, 2008; pp. 677–685.
2. Hufkens, K.; Scheunders, P.; Ceulemans, R. Ecotones in vegetation ecology: Methodologies and definitions revisited. *Ecol. Res.* **2009**, *24*, 977–986. [[CrossRef](#)]
3. Wang, X.Q.; Zhao, C.J. Sand surface change and natural species entrance in straw barrier system in Gurbantunggut Desert, Xinjiang, China. *Arid Land Geogr.* **2002**, *25*, 201–207. (In Chinese)

4. Xu, J.; Gu, H.; Meng, Q.; Cheng, J.; Liu, Y.; Jiang, P.; Sheng, J.; Deng, J.; Bai, X. Spatial pattern analysis of Haloxylon ammodendron using UAV imagery—A case study in the Gurbantunggut Desert. *Int. J. Appl. Earth Obs. Geoinf.* **2019**, *83*, 101891. [[CrossRef](#)]
5. Huang, P.Z.; Liu, Z.J.; Cui, W.C. A preliminary study on water harvesting afforestation of Haloxylon ammodendron. *Xinjiang Agric. Sci.* **1985**, *6*, 23–25. (In Chinese)
6. Li, C.J.; Lei, J.Q.; Zhao, Y. Effect of saline water irrigation on soil development and plant growth in the Taklimakan Desert Highway Shelterbelt. *Soil. Till. Res.* **2015**, *146*, 99–107. [[CrossRef](#)]
7. Zhou, Z.B.; Xu, X.W. Absorption characteristics of ions in three species of shrubs of the artificially-planted greenbelts in the hinterland of the Taklamakan Desert. *Arid Zone Res.* **2002**, *19*, 49–52. (In Chinese)
8. Li, C.; Shi, X.; Mohamad, O.A.; Gao, J.; Xu, X.; Xie, Y. Moderate irrigation intervals facilitate establishment of two desert shrubs in the Taklimakan Desert Highway Shelterbelt. *PLoS ONE* **2017**, *12*, e0180875. [[CrossRef](#)] [[PubMed](#)]
9. Wang, X.Q.; Wang, T.; Jiang, J. On the sand surface stability in the southern part of the Gurbantunggut Desert. *Sci. China Ser. D Earth Sci.* **2005**, *48*, 778–785. [[CrossRef](#)]
10. Xiao, D.Z.; Hu, Y.K. A preliminary study on the runoff and its utilization of the crevasse crack ground (A case study of Mo-suowan pilot zone). *Arid Land Geogr.* **1985**, *8*, 28–34. (In Chinese)
11. Li, Y.F.; Yang, G. Studies on the moisture balance of Haloxylon ammodendron sand-break Forest: The Moisture State of Haloxylon ammodendron autumn irrigated sand-break forest. *Arid Zone Res.* **1996**, *13*, 57–62. (In Chinese)
12. Chen, Q.M.; Luo, Q.H.; Ning, H.S.; Zhao, C.Y.; Duan, W.B. Characteristics of main stand layer and regeneration layer of Haloxylon ammodendron plantations at different ages on the southern edge of the Gurbantunggut Desert, Northwest China. *Chin. J. Appl. Ecol.* **2017**, *28*, 739–747.
13. Greig-Smith, P. Pattern in Vegetation. *J. Ecol.* **1979**, *67*, 755. [[CrossRef](#)]
14. Bagchi, R.; Henrys, P.A.; Brown, P.E.; Burslem, D.F.R.P.; Diggle, P.; Gunatilleke, C.V.S.; Gunatilleke, I.A.U.N.; Kassim, A.R.; Law, R.; Noor, S.; et al. Spatial patterns reveal negative density dependence and habitat associations in tropical trees. *Ecology* **2011**, *92*, 1723–1729. [[CrossRef](#)] [[PubMed](#)]
15. Velázquez, E.; Paine, C.E.T.; May, F.; Wiegand, T. Linking trait similarity to interspecific spatial associations in a moist tropical forest. *J. Veg. Sci.* **2015**, *26*, 1068–1079. [[CrossRef](#)]
16. Zhang, J.T. Analysis of spatial point pattern for plant species. *Acta Phytoecol. Sin.* **1998**, *22*, 344–349.
17. Li, C.-J.; Lei, J.-Q.; Shi, X.; Liu, R. Scale Dependence of Soil Spatial Variation in a Temperate Desert. *Pedosphere* **2014**, *24*, 417–426. [[CrossRef](#)]
18. Couteron, P.; Kokou, K. Woody vegetation spatial patterns in a semi-arid savanna of Burkina Faso, West Africa. *Plant Ecol.* **1997**, *132*, 211–227. [[CrossRef](#)]
19. Barot, S.; Gignoux, J.; Menaut, J. Demography of a savanna palm tree: Predictions from comprehensive spatial pattern analyses. *Ecology* **1999**, *80*, 1987–2005. [[CrossRef](#)]
20. Stoll, P.; Bergius, E. Pattern and process: Competition causes regular spacing of individuals within plant populations. *J. Ecol.* **2005**, *93*, 395–403. [[CrossRef](#)]
21. Zheng, Y.; Zhao, W.Z.; Zhang, G.F. Spatial analysis of a Haloxylon ammodendron plantation in an oasis-desert ecotone in the Hexi corridor, northwestern China. *Forests* **2017**, *8*, 200. [[CrossRef](#)]
22. Malkinson, D.; Tielbörger, K. What does the stress-gradient hypothesis predict? Resolving the discrepancies. *Oikos* **2010**, *119*, 1546–1552. [[CrossRef](#)]
23. Hao, H.-M.; Huang, Z.; Lu, R.; Jia, C.; Liu, Y.; Liu, B.-R.; Wu, G.-L. Patches structure succession based on spatial point pattern features in semi-arid ecosystems of the water-wind erosion crisscross region. *Glob. Ecol. Conserv.* **2017**, *12*, 158–165. [[CrossRef](#)]
24. Gross, K. Positive interactions among competitors can produce species-rich communities. *Ecol. Lett.* **2008**, *11*, 929–936. [[CrossRef](#)] [[PubMed](#)]
25. Konings, A.G.; Dekker, S.C.; Rietkerk, M.; Katul, G.G. Drought sensitivity of patterned vegetation determined by rainfall-Land surface feedbacks. *J. Geophys. Res.* **2011**, *116*, 1–15. [[CrossRef](#)]
26. Bestelmeyer, B.T.; Duniway, M.C.; James, D.K.; Burkett, L.M.; Havstad, K.M. A test of critical thresholds and their indicators in a desertification-prone ecosystem: More resilience than we thought. *Ecol. Lett.* **2012**, *16*, 339–345. [[CrossRef](#)]
27. Kulasova, A.; Blazkova, S.; Beven, K.; Řezáčová, D.; Cajthaml, J. Vegetation pattern as an indicator of saturated areas in a Czech headwater catchment. *Hydrol. Process.* **2014**, *28*, 5297–5308. [[CrossRef](#)]
28. Schleicher, J.; Wiegand, K.; Ward, D. Changes of woody plant interaction and spatial distribution between rocky and sandy soil areas in a semi-arid savanna, South Africa. *J. Arid. Environ.* **2011**, *75*, 270–278. [[CrossRef](#)]
29. Song, Y.Y.; Li, Y.Y.; Zhang, W.H. Analysis of spatial pattern and spatial association of Haloxylon ammodendron population in different developmental stages. *Acta Ecol. Sin.* **2010**, *30*, 4317–4327. (In Chinese)
30. Browning, D.M.; Franklin, J.; Archer, S.R.; Gillan, J.K.; Guertin, D.P. Spatial patterns of grassland–shrubland state transitions: A 74-year record on grazed and protected areas. *Ecol. Appl.* **2014**, *24*, 1421–1433. [[CrossRef](#)]
31. Li, Y.; Xu, H. Water and Carbon balances of Haloxylon ammodendron: Integrated study and physiological, plant and community level. *Arid Land Geogr.* **2008**, *31*, 313–323.
32. Field, C.B.; Barros, V.R.; Dokken, D.J. *Intergovernmental Panel on Climate Change. Summary for Policymakers//Climate Change 2014-Impacts, Adaptation and Vulnerability. Part A: Global and Sectoral Aspects*; Cambridge University Press: Cambridge, UK, 2014; pp. 1–32.

33. Wang, X.Q.; Zhang, Y.M.; Jiang, J. Variation pattern of soil water content in longitudinal dune in the southern part of Gurbantünggüt desert: How snow melt and frozen soil change affect the soil moisture. *J. Glaciol. Geocryol.* **2006**, *28*, 262–268. (In Chinese)
34. Dai, Y.; Zheng, X.-J.; Tang, L.-S.; Li, Y. Stable oxygen isotopes reveal distinct water use patterns of two Haloxylon species in the Gurbantonggut Desert. *Plant Soil* **2015**, *389*, 73–87. [[CrossRef](#)]
35. Cheng, C.D.; Zhang, L.Y.; Hu, W.K. The basic characteristics of plant communities, flora and their distribution in the sandy district of Gurbantungut. *Acta Phytoecol. Geobot. Sin.* **1983**, *7*, 89–98. (In Chinese)
36. Ning, H.S.; Luo, Q.H.; Ji, X.M.; Lei, C.Y. Assessment on ecosystem service value of Haloxylon ammodendron forest in Xinjiang. *Ecol. Sci.* **2017**, *36*, 74–81. (In Chinese)
37. Luo, Q.H.; Chen, Q.M.; Ning, H.S.; Zhao, C.Y. Chronosequence-based population structure and natural regeneration of Haloxylon ammodendron plantation in the southern edge of the Gurbantungut Desert, Northwestern China. *Russ. J. Ecol.* **2017**, *48*, 364–371. [[CrossRef](#)]
38. Shao, Y.Y.; Zhang, Y.Q.; Wu, X.Q.; Charles, P.A.; Zhang, J.T.; Qin, S.G.; Wu, B. Relating historical vegetation cover to aridity patterns in the greater desert region of northern China: Implications to planned and existing restoration projects. *Ecol. Indic.* **2018**, *89*, 528–537. [[CrossRef](#)]
39. Chen, F.L.; Zheng, X.R.; He, X.L.; Yang, G.; Liu, B. Change of groundwater depth and impact factors in Mosuowan irrigation district during 1998–2007. *Eng. J. Wuhan Univ.* **2011**, *44*, 317–320. (In Chinese)
40. Jiang, L. Analysis on groundwater characteristics at Mosuowan irrigation district of the Manas river basin. *Ground water* **2016**, *38*, 1–3. (In Chinese)
41. Li, C.J.; Li, Y.; Ma, J. Spatial heterogeneity of soil chemical properties at fine scales induced by Haloxylon ammodendron (Chenopodiaceae) plants in a sandy desert. *Ecol. Res.* **2011**, *26*, 385–394. [[CrossRef](#)]
42. Zhang, Y.; Li, Y.; Xie, J.-B. Fixed allocation patterns, rather than plasticity, benefit recruitment and recovery from drought in seedlings of a desert shrub. *AoB Plants* **2016**, *8*, 1–11. [[CrossRef](#)]
43. Dale, M.R.T.; Fortin, M.J. *Spatial Analysis: A Guide for Ecologists*, 2nd ed.; Cambridge University Press: Cambridge, UK, 2014; p. 382.
44. Zuo, X.A.; Zhao, X.Y.; Zhao, H.L. Spatial heterogeneity of vegetation characteristics in the processes of degraded vegetation restoration in Horqin Sandy Land, northern China. *Ecol. Environ. Sci.* **2010**, *19*, 1513–1518. (In Chinese)
45. Rundel, P.W. Community Structure and Stability in the Giant Sequoia Groves of the Sierra Nevada, California. *Am. Midl. Nat.* **1971**, *85*, 478. [[CrossRef](#)]
46. Jia, Z.Q.; Lu, Q. *Haloxylon Ammodendron*; China Environmental Science Press: Beijing, China, 2005.
47. Pillay, T.; Ward, D. Spatial pattern analysis and competition between Acacia karroo trees in humid savannas. *Plant Ecol.* **2012**, *213*, 1609–1619. [[CrossRef](#)]
48. Diggle, P.J. *Statistical Analysis of Spatial and Spatio-Temporal Point Patterns*, 3rd ed.; CRC Press: Boca Raton, FL, USA, 2013; pp. 1–5.
49. Ramon, P.; De La Cruz, M.; Zavala, I.; Zavala, M.A. Factors influencing the dispersion of *Arceuthobium oxycedrii* in Central Spain: Evaluation with a new null model for marked point patterns. *For. Pathol.* **2016**, *46*, 610–621. [[CrossRef](#)]
50. Besag, J. Contribution to the discussion of Dr. Ripley's paper. *J. R. Stat. Soc. Ser. B* **1977**, *39*, 193–195.
51. Ripley, B.D. Modelling Spatial Patterns. *J. R. Stat. Soc. Ser. B* **1977**, *39*, 172–192. [[CrossRef](#)]
52. Goreaud, F.; Pélissier, R. On explicit formulas of edge effect correction for Ripley's K-function. *J. Veg. Sci.* **1999**, *10*, 433–438. [[CrossRef](#)]
53. Wiegand, T.; Moloney, K.A. Rings, circles, and null-models for point pattern analysis in ecology. *Oikos* **2004**, *104*, 209–229. [[CrossRef](#)]
54. Duncan, R.P.; Stewart, G.H. The temporal and spatial analysis of tree age distributions. *Can. J. For. Res.* **1991**, *21*, 1703–1710. [[CrossRef](#)]
55. Baddeley, A.; Turner, R.; Hazelton, J.M. Residual analysis for spatial point processes. *J. R. Stat. Soc.* **2005**, *67*, 617–666. [[CrossRef](#)]
56. Wu, X.; Zheng, X.-J.; Li, Y.; Xu, G.-Q. Varying responses of two Haloxylon species to extreme drought and groundwater depth. *Environ. Exp. Bot.* **2019**, *158*, 63–72. [[CrossRef](#)]
57. Li, J.J.; Xue, B.R.; Chai, Z.Z. Quantity dynamics and distribution pattern for Haloxylon ammodendron population of the desert-oasis ecotone in Minqin county of Gansu province, china. *J. Northeast For. Univ.* **2013**, *41*, 27–31.
58. Wu, X.; Zheng, X.-J.; Yin, X.-W.; Yue, Y.-M.; Liu, R.; Xu, G.-Q.; Li, Y. Seasonal variation in the groundwater dependency of two dominant woody species in a desert region of Central Asia. *Plant Soil* **2019**, *444*, 39–55. [[CrossRef](#)]
59. Zheng, X.J.; Li, Y.; Wu, X.; Xu, G.Q. Deepening Rooting Depths Improve Plant Water and Carbon Status of A Xeric Tree during Summer Drough. *Forests* **2019**, *10*, 592. [[CrossRef](#)]
60. Zhang, Y.; Xie, J.B.; Li, Y. Effects of increasing root carbon investment on the mortality and resprouting of Haloxylon ammodendron seedlings under drought. *Plant Biol.* **2016**, *19*, 191–200. [[CrossRef](#)] [[PubMed](#)]
61. Ponge, J.F.; Andre, J.; Zackrisson, O.; Bernier, N.; Nilsson, M.C.; Gallet, C. The forest regeneration puzzle. *BioScience* **1998**, *48*, 523–530.
62. Tirado, R.; Pugnaire, F.I. Shrub spatial aggregation and consequences for reproductive success. *Oecologia* **2003**, *136*, 296–301. [[CrossRef](#)] [[PubMed](#)]

63. Zhou, C.B.; Song, Y.Y. Influence of different longitudinal dune positions in the Gurbantunggut Desert on the reproduction of *Haloxylon ammodendron* seedlings. *Appl. Ecol. Environ. Res.* **2015**, *13*, 99–113. (In Chinese)
64. Halik, Ü.; Aishan, T.; Betz, F.; Kurban, A.; Rouzi, A. Effectiveness and challenges of ecological engineering for desert riparian forest restoration along China's largest inland river. *Ecol. Eng.* **2019**, *127*, 11–22. [[CrossRef](#)]
65. Song, C.W.; Jiang, J.; Fu, H.F.; Chen, J.J. Soil moisture in plantation area and its affecting factors in the Gurbantonggut desert. *Arid Land Geogr.* **2009**, *32*, 704–710. (In Chinese)
66. Xu, H.; Li, Y.; Xu, G.; Zou, T. Ecophysiological response and morphological adjustment of two Central Asian desert shrubs towards variation in summer precipitation. *Plant Cell Environ.* **2007**, *30*, 399–409. [[CrossRef](#)] [[PubMed](#)]
67. Xu, G.-Q.; McDowell, N.G.; Li, Y. A possible link between life and death of a xeric tree in desert. *J. Plant Physiol.* **2016**, *194*, 35–44. [[CrossRef](#)] [[PubMed](#)]